A Switched System Modeling Approach for a Pneumatic Muscle Actuator

G. Andrikopoulos, J. Arvanitakis, S. Manesis
Department of Electrical and Computer Engineering
University of Patras
Rio, Greece 26500
Email: andrikopg(arvanitakis)stam.manesis@ece.upatras.gr

G. Nikolakopoulos
Department of Electrical, Computer and Space Engineering
Luleå University of Technology
Luleå, Sweden 97187
Email: george.nikolakopoulos@ltu.se

***Abstract*—The aim of this article is to present a switched system approach for the dynamic modeling of Pneumatic Muscle Actuators (PMAs). PMAs are highly non-linear pneumatic actuators where their elongation is proportional to the interval pressure. During the last two decades, various modeling approaches have been presented that describe the behavior of PMAs. While most mathematical models are characterized by simplicity and accuracy in describing the attributes of PMAs, they are limited to static performance analysis. Static models are proven to be insufficient for real time control applications, thus creating the need for the development of dynamic PMA models. A collection of experimental and simulation results are being presented that prove the efficiency of the proposed approach.**

I. Introduction

The Pneumatic Muscle Actuator [1], also known as the McKibben Pneumatic Artificial Muscle (PMA) [2–5], Fluidic Muscle [6] or the Biomimetic Actuator [7], is a tube–like actuator that is characterized by a decrease in the actuating length when pressurized [8–11]. Best known member of this family is the McKibben–Muscle, which was first invented in 1950s by the physician, Joseph L. McKibben and has been utilized as an orthotic appliance for polio patients [2]. The first commercialization of PMAs has been done by the Bridgestone Rubber Company of Japan in the 1980s. PMAs are significantly light actuators, which are characterized by smooth, accurate and fast response and also are able to produce a significant force when fully stretched.

Typical manufacturing of a PMA can be found as a long synthetic or natural rubber tube, wrapped inside man-made netting, such as Kevlar, at predetermined angle. Protective rubber coating surrounds the fibber wrapping and appropriate metal fittings are attached at each end. The PMA converts pneumatic power to pulling force and has many advantages over conventional pneumatic cylinders, such as high force to weight ratio, variable installation possibilities, no mechanical parts, lower compressed-air consumption and low cost [12].

The PMA, when compressed, air is applied to the interior of the rubber tube, it contracts in length and expands radially. As the air exits the tube, the inner netting acts as a spring that restores the tube in its original form. This actuation reminds the operation of a single acting pneumatic cylinder with a spring return, while this reversible physical deformation, during the contraction and expansion of the muscle, results in an almost linear motion. Typical types of PMAs and the corresponding naming are depicted in Figure 1 [13].

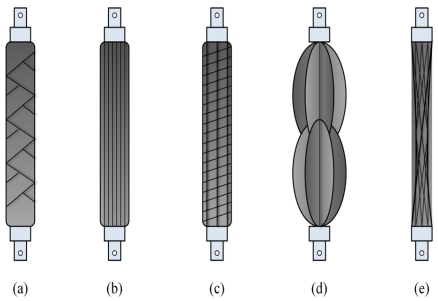

Fig. 1. Various types of PMAs, (a) McKibben Muscle/Braided Muscle, (b) Pleated Muscle, (c) Yarlott Netted Muscle, (d) ROMAC Muscle and (e) Paynter Hyperboloid Muscle.

Various modeling approaches have been presented in the scientific field of PMA–modeling. These approaches, although incorporate basic and more detailed analysis of PMAs, in the area of PMA applications, most of the models are based on the geometry of the PMA, mainly due to the models simplicity and great relativity to the experimental behavior [14], while the model is being derived based on a fundamental operation point (when the muscle is not pressurized). Among these models, the Chou and Hannaford model [15] and the Tondu and Lopez model [16] have been widely utilized in most of PMA applications.

The main novelty of this article is to propose a switching system approach for the modeling of the nonlinear PMAs, based on multiple linear systems, derived from multiple corresponding operation points. Based on this approach, the larger the number of the linear system is, the better the non–linear model, is approximated by the set of switched linear models. The state of the actuator's elongation rules the switchings while this scheme allows for the future application of novel control schemes, e.g. switching controllers.

The rest of the article is structured as it follows. In Section II the fundamental modeling for static and dynamic PMA performance will be presented, while in Section III the switching system modeling approach will be analysed. In Section IV, experimental estimation of the PMA phenomeno-

logical model's parameters and the validation of the dynamic model accompanied by simulation results will be presented. Finally the conclusions will be drawn in Section V.

II. Fundamental modeling for PMA performance

A. Static Modeling

The Chou and Hannaford model, is the most simple geometrical model for a static performance of a PMA. The proposed model is valid under the following assumptions: a) the actuator is cylindrical in shape, b) the threads in the sheath are inextensible and always in contact with the outside diameter of the latex bladder, c) frictional forces between the tubing and the sheath and between the fibers of the sheath are negligible, and d) latex tubing forces are negligible. With this approach the PMA actuator can be modelled as a cylinder, depicted in Figure 2, with a length L, thread length b, diameter D, and number of thread turns n. The angle θ is defined as the angle of the threads with the longitudinal axis [17].

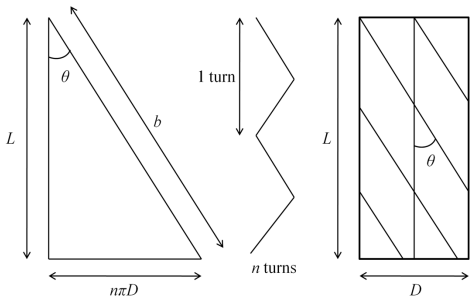

Fig. 2. Simplified Geometrical Model of PMA.

When the PMA actuator inflates, D and L change, n and b remain constant, while the expressions for the PMA's length and diameter can be formulated as:

$$L = b\cos\theta, \quad D = b\frac{\sin\theta}{n\pi} \tag{1}$$

where the thread length can be calculated as:

$$b = \left(L^2 + D^2 n^2 \pi^2\right)^{1/2} \tag{2}$$

Equation (2) is referred in the literature as the geometric relationship for the PMA, while its volume is provided by:

$$V = \frac{b^3 \cos\theta \sin^2\theta}{4n^2\pi} \tag{3}$$

Utilizing the energy conservation principle, the PMA simple geometric force F_g can be calculated as the gauge pressure multiplied by the change in volume with respect to length (this model can also be found in [17]):

$$F_g = \frac{pb^2(3cos^2\theta - 1)}{4\pi n^2} \tag{4}$$

Another simple and widely utilized geometrical model of PMA is that of Tondu and Lopez [16]. Based on this approach and by: a) utilizing similar geometric description of the muscle with [15], b) assuming inextensibility of the mesh material, and c) angle changes during the alteration of the PMAs length, the following mathematical modeling approach can be derived, based on the theorem of virtual work [18]:

$$F(\epsilon, P) = \pi r_0^2 \cdot P[a(1-\epsilon)^2 - \beta] \tag{5}$$

where:

$$\epsilon = \frac{l_0 - l}{l_0}, \quad d0 \le \epsilon \le \epsilon_{max}, \quad a = \frac{3}{\tan^2\theta_0}, \quad \beta = \frac{1}{\sin^2\theta_0} \tag{6}$$

In equations (5) and (6), r_0 is the nominal inner radius, l the length of the muscle, l_0 the initial nominal length, P the pressure and θ_0 is the initial angle between the membrane fibres and the muscle axis, while this model can also be found in [19]. A disadvantage of the model is that its design is based on the hypothesis of a continuously cylindrical–shaped muscle, whereas it takes a conic shape at both ends when it contracts. Consequently, the more the muscle contracts, the more its active part decreases. This phenomenon affects the actual maximum contraction, as theoretically it is smaller than that expected from (5) [20]. For improving equation (5), an empirical factor k has been added [16] to account for the end deformation of the PMA:

$$F(\epsilon, P) = \pi r_0^2 \cdot P[a(1-k\epsilon)^2 - \beta] \tag{7}$$

where again: $0 \le \epsilon \le \epsilon_{max}$ and $\epsilon_{\max}$ is provided from:

$$\epsilon_{\max} = (1/k)(1 - \sqrt{\beta/a}) \tag{8}$$

Inserted in this way within the considered static model, the parameter k does not modify the value of the maximum force given at zero contraction. This is in concordance with the conducted experiment since the PMA has a cylindrical shape only when its contraction ratio is zero. Furthermore, the parameter k allows adapting the model maximum contraction ratio given by (8) to the experimental data. Thus, it tunes the "slope" of the considered static model. In addition it has been established two options for the selection of the parameter k: a) a constant value which may vary depending on the material that the muscle made of, and b) the parameter k depends on the pressure in the muscle at any given time.

B. Dynamic Modeling

Although the geometrical models are characterized by simplicity, they are not beneficial for real time control applications because they strictly describe the static behavior of PMAs and analyze their performance in quasi-static state. The PMA geometric structure variables are inaccessible and difficult to obtain from experimental data, thus, creating the need for the development of dynamic PMA models. More recently, a phenomenological modeling approach describes accurately the dynamics of PMAs using a model with three elements. Specifically, during expansion, PMA experiences viscoelastic resistance which can be modeled as a damping and spring element. Thus, in the phenomenological model, the PMA is being considered as a parallel pattern that consists of a spring element, a damping element and a contractile element as it is presented in Figure 3 [21].

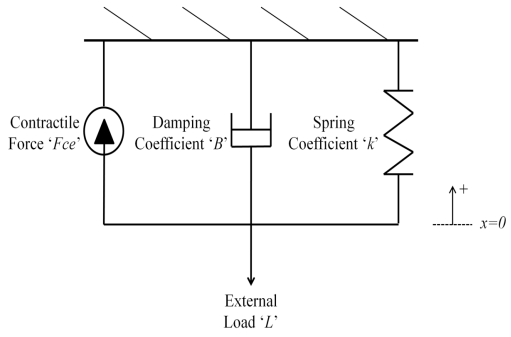

Fig. 3. Phenomenological Model of PMA.

This model corresponds to the system of a PMA on the vertical position with one end fixed and an external load L attached to the other end. The differential equation that describes the overall system is the following:

$$M\ddot{x} + B\dot{x} + Kx = F_{ce} - L \tag{9}$$

where $x \in \Re^+$ is the displacement of the PMA, M is the mass of the muscle, P is the control pressure, L is the external load, K is the spring constant, B is the damping coefficient and F_{ce} is the force exerted by the muscle as described in [16] and it is provided by the following equation:

$$F_{ce} = \pi r_0^2 \left(a(1 - \frac{x}{l_0})^2 - b \right) P \tag{10}$$

As it has been indicated in [21], at a steady state L both damping and spring coefficients are polynomial expressions of pressure P and can be formulated as:

$$B(P) = \sum_{i=0}^{n} b_i P^i \tag{11}$$

$$K(P) = \sum_{i=0}^{n} k_i P^i \tag{12}$$

with $i,\ n \in \mathbb{Z}^+$, n the order of the approximated polynomial, and $b_i,\ k_i \in \Re^2$ are the polynomial coefficients correspondingly. From equations (11) and (12) it can be observed that the higher the order, the better the approximation is with a trade off in the complexity of the non–linear system.

III. Switching System Modeling Approach

By combining equations in (9) and (10), the full non–linear state space equation that describes the elongation of the PMA, can be cast as:

$$\ddot{x} + \frac{B(P)}{M}\dot{x} + \frac{K(P)}{M}x - \frac{\pi r_0^2}{M} P \left[a(1 - \frac{x}{l_0})^2 - b \right] + \frac{1}{M} L = 0 \tag{13}$$

The operating points x_j^{op}, with $j = \{0, \ldots, N\}$ and $N \in \mathbb{Z}^+\}$, depend on the applied nominal pressure P_j^{op}, under the assumption of a constant load experiment. By zeroing the terms $\ddot{x} = \dot{x} = 0$, equation (13) yields:

$$\frac{K}{M} x_j^{op} - \frac{\pi r_0^2}{M} P_j^{op} \left[a(1 - \frac{x_j^{op}}{l_0})^2 - b \right] + \frac{1}{M} L = 0 \tag{14}$$

which is the equality that all the equilibrium points $[x_j^{op},\ P_j^{op}]$ should satisfy. This means that a nominal pressure P_j^{op} should be applied to the PMA, if its length is to be maintained at a distance x_j^{op} from its un–stretched position.

The linearized equations of motion for the PMA, around multiple equilibrium points j can be formulated by considering small perturbations around the variables x and P, or considering $x = x_j^{op} + \delta x$ and $P = P_j^{op} + \delta P$. By applying this linearization approach on equation (13), the state space representation:

$$\mathbf{x} = [\delta x,\ \delta \dot{x}]^T \in \mathcal{X} \subseteq \Re^2$$

for the elongation of the PMA, under the following control vector:

$$\mathbf{u} = [\delta P,\ 0]^T \in \mathcal{U} \subseteq \Re^2$$

can be mathematically formulated as it follows:

$$\dot{\mathbf{x}} = \mathbf{A_j}\mathbf{x} + \mathbf{B_j}\mathbf{u}, \tag{15}$$

where the state space matrices are defined as:

$$\mathbf{A_j} = \begin{bmatrix} 0 & 1 \\ -\frac{k_j^{op}}{M} - \frac{2\pi r_0^2 a}{M l_0} P_j^{op} (1 - \frac{x_j^{op}}{l_0}) & -\frac{b_j^{op}}{M} \end{bmatrix} \tag{16}$$

$$\mathbf{B_j} = \begin{bmatrix} 0 & 0 \\ \frac{\pi r_0^2}{M}[a(1 - \frac{x_j^{op}}{l_0})^2 - b] & -\frac{1}{M} \end{bmatrix} \tag{17}$$

and the sets $\mathcal{X}$ and $\mathcal{U}$ specify state and input operating regions that contain the operating points in their interior (middle point).

The system described in (15) is switched, as j belongs to a finite set of indexes and N denotes the number of switched systems, with the state x to act as the switching rule. If Σ is the polytope that contains all the switching systems, defined by the switching vertices $[\mathbf{A}_j,\ \mathbf{B}_j]$, it can be notated as:

$$\text{Co}\{[\mathbf{A}_1\ \mathbf{B}_1], \cdots, [\mathbf{A}_N\ \mathbf{B}_N]\} \tag{18}$$

where the notation Co denotes the convex hull of the set, and any $[\mathbf{A}_j,\ \mathbf{B}_j]$ within the convex set Σ, is a linear combination of:

$$[\mathbf{A}_j,\ \mathbf{B}_j] = \sum_{j=1}^{N} a_j [\mathbf{A}_j, \mathbf{B}_j],\ \sum_{j=1}^{N} a_j = 1,\ \ 0 \le a_j \le 1 \tag{19}$$

IV. Model Validation

A. Experimental Contraction Study

In order to calculate and estimate the efficiency of the proposed switched system modeling approach, values for B and K elements are required. For this reason, a simple experiment for a rough estimation of said values was conducted. The experimental setup that was constructed for the extraction of B and K elements, as provided in (11) and (12), respectively, is depicted in Figure 4. The setup consists of a pneumatic muscle actuator on the vertical position with one end fixed, a proportional pressure regulator and a linear position sensor.

The PMA utilized in this test–bed was a Festo MXAM–40–AA–DMSP–40–305N–AM–CM Fluidic Muscle with 40mm of

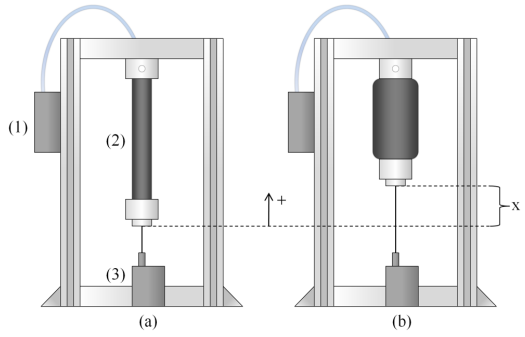

Fig. 4. PMA Experimental Setup: (1) Proportional Pressure Regulator, (2) Pneumatic Muscle Actuator, (3) Linear Position Sensor.

internal diameter and 305mm of nominal length. The PMA is on the vertical position and has its upper end clumped. A Festo VPPM-6F-L-1-F-0L6H-V1N Proportional Pressure Regulator was used to regulate the supply and pressure of the compressed air supplied into the PMA. Moreover an ASM WS12 cable actuated linear position sensor with analogue output was utilized to measure the PMAs displacement in the vertical axis. The control of the setup operation, as well as the data acquisition, was achieved by utilizing a National Instruments USB–6215 Data Acquisition Card. The dynamic experiments in this study were conducted on the test system utilizing vertical layout with steady state L. With no additional load attached to the PMA, and considering that the upper end of the muscle is clumped, half of its mass is supported; the L load is constant and equals half the weight of the PMA.

Considering the previous studies in [22] the method, for the case of estimating the damping and spring coefficients only, could be simplified by ignoring the inertial term $M\ddot{x}$ of the phenomenological model, and considering it as a first order system. Given that a rough estimation - and not a accurate identification - of the B, K parameters is needed for the further development of the switched modeling approach, this assumption has no major impact in the simulation studies. Thus, equation (9) becomes:

$$B\dot{x} + Kx = F_{ce} - L \tag{20}$$

For step changes in pressure and $F_{ce} > L$, the solution of the above equation has been calculated as [22]:

$$x(t) = \frac{F_{ce} - L}{K}\left((1 - e^{-\frac{K}{B}t}\right) = x_{max}\left((1 - e^{-\frac{K}{B}t}\right) \tag{21}$$

where Δx_{max} is the maximum contraction at steady state. The above equation relates the damping B and spring K coefficients with the displacement x, the contraction force F_{ce} and the load L. To provide independent estimates of the model elements as functions of the pressure P, a contraction study was conducted to parameterize the damping $B(P)$ and the spring constant $K(P)$ responses [21] with the utilization of the theoretical solution described above. Successive inflations of the PMA were conducted, with pressures between 0-6bar (0-600kPa) by 0.5bar increments. The Force coefficients F_{ce} at each pressure were estimated from (10) for $x = x_{max}$, while the spring element K was estimated at each state by the following equation:

$$K = \frac{F_{ce} - L}{x_{max}} \tag{22}$$

The obtained results for: a) the experimental dependency of the spring coefficient K to the applied pressure P, b) the linear approximation of K as a function of P, and c) the switched linear approximation of K that will be utilized in the following subsection, are displayed in Figure 5. as it has been observed in [22] and experimentally evaluated in the provided results, the dependency of K and B from P is different than the one in higher pressures. This is one of the reasons that PMA are usually operated in higher pressures.

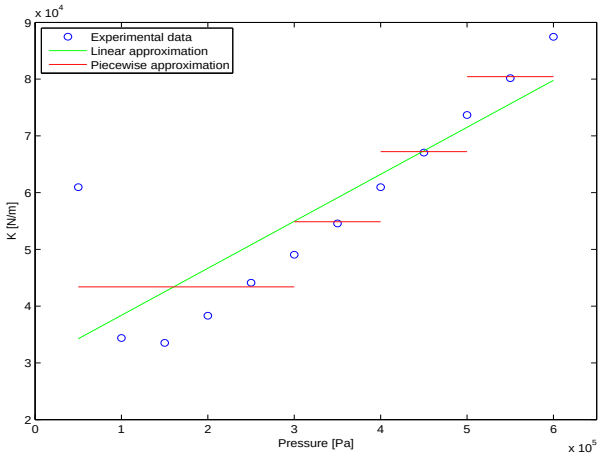

Fig. 5. Spring Coefficient Estimates for Pressures 0-6bar.

From equation (21), the time constant of the displacement response is equal to:

$$\tau = \frac{B}{K} \tag{23}$$

Based on these displacement responses the corresponding time constants were estimated. Then, the damping element B was calculated at each state using equation (23). In Figure 6 it is displayed: a) the dependency of the damping coefficient B experimental measurements to the pressure P, b) the linear approximation of B as a function of pressure, and c) the the switched linear approximation approximation that will be utilized in the next subsection.

B. Simulation Results

Having estimated the relations of B(P) and K(P) in the subsection 4.1, this section will focus on the switched model verification. The number of the switched systems has been selected as $N = 4$, which corresponds to 4–linearization points as depicted in Table I

The validity of the aforementioned switched system modeling when compared with the non–linear model, will be provided based on the consideration of 2^{nd}–order (linear) polynomials for the $B(P)$ and $K(P)$, or considering $B(P) =$

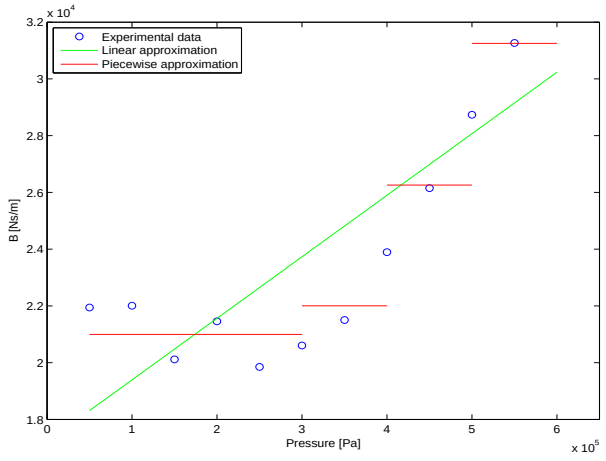

Fig. 6. Damping Coefficient Estimates for Pressures 0-6bar.

TABLE I
PMA LINEARIZATION POINTS

N	Parameters	Linearization Regions
1	$\mathbf{x}^\circ = [0.0399,\ 0]$	$x \in [0,\ 0.0581]$
2	$\mathbf{x}^\circ = [0.0622,\ 0]$	$x \in [0.0581,\ 0.0657]$
3	$\mathbf{x}^\circ = [0.0688,\ 0]$	$x \in [0.0657,\ 0.0715]$
4	$\mathbf{x}^\circ = [0.0739,\ 0]$	$x \in [0.0715,\ 0.076]$

$b_0 + b_1 P$ and $K(P) = k_0 + k_1 P$. In all the simulations, that will be presented in the sequence, the step response of the PMA, modeled as a switched system, will be presented when inflamed with various pressures. It should be noted that in these Figures, with solid line we present the response of the non–linear system and with dash–dotted line, the response of the switched linear system.

In the first simulation case, the PMA is inflated by a constant pressure $P = 3.1bar$ and the responses of the switched and the non–linear system are depicted in Figure 7. Under this applied pressure, the PMA achieves to reach a maximum elongation at $x = 0.0589m$ in the non–linear case, and $x = 0.0599m$ in the switched case, that gives a total steady state error of 1.7% . In the examined test–case, it should be noted that $N = 2$ switched systems have been utilized ($N = 1,\ 2$), as it has been displayed in Figure 8.

In the second simulation case, the PMA is inflated by a constant pressure $P = 4.8bar$ and the responses of the switched and the non–linear system are depicted in Figure 9. Under this applied pressure, the PMA achieves to reach a maximum elongation at $x = 0.0704m$ in the non–linear case, and $x = 0.07m$ in the switched case, that gives a total steady state error of 0.5% . In the examined test–case, the system had to switch among $N = 3$ switched systems ($N = 1,\ 2,\ 3$), as it has been displayed in Figure 10.

In the final simulation case, the PMA is inflated by a constant pressure of $P = 6bar$ and the responses of the switched and the non–linear system are depicted in Figure 11. Under this applied pressure, the PMA achieves to reach a maximum elongation at $x = 0.076m$ in the non–linear case,

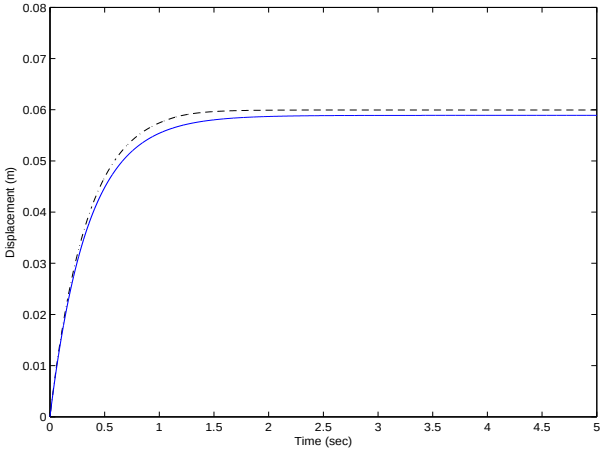

Fig. 7. Step Response for pressure $P = 3.4bar$

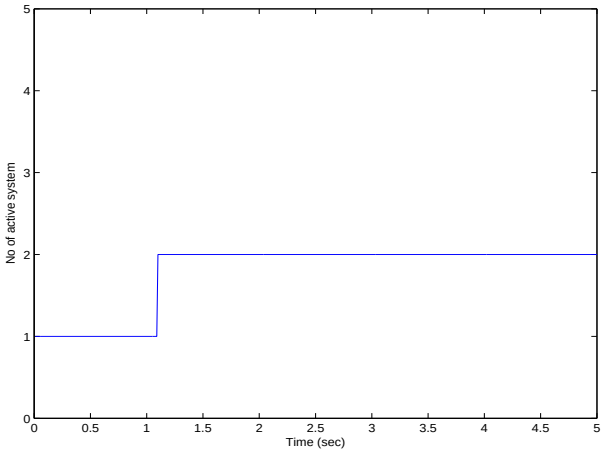

Fig. 8. Switched system activation for pressure $P = 3.1bar$

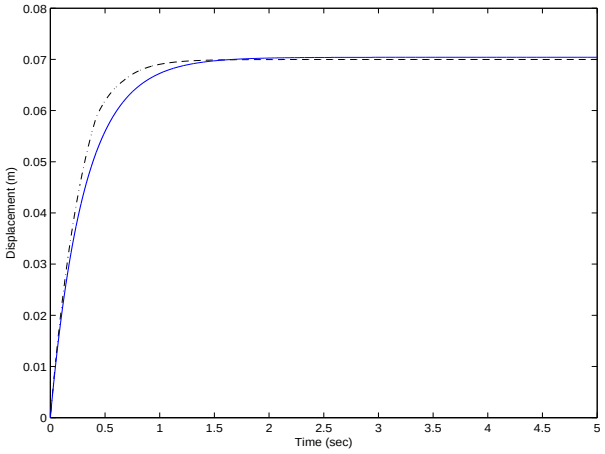

Fig. 9. Step Response for pressure $P = 4.8bar$

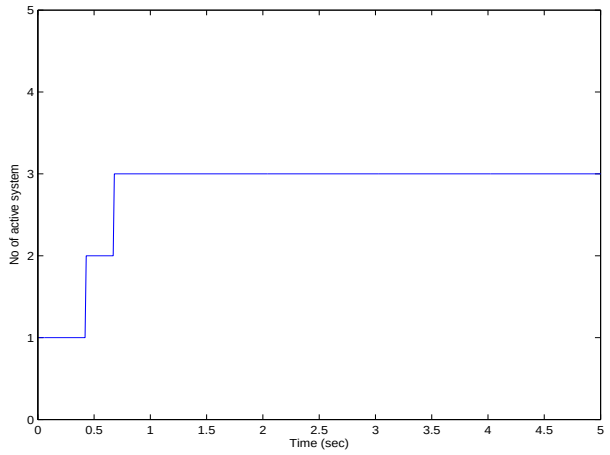

Fig. 10. Switched system activation for pressure $P = 4.8bar$

and $x = 0.0753m$ in the switched case, that gives a total steady state error of 0.92% . In the examined test–case, it should be noted that all the utilized switched systems have been utilized ($N = 1,\ 2,\ 3,\ 4$), as it has been presented in Figure 12. From all the previous results, it should be

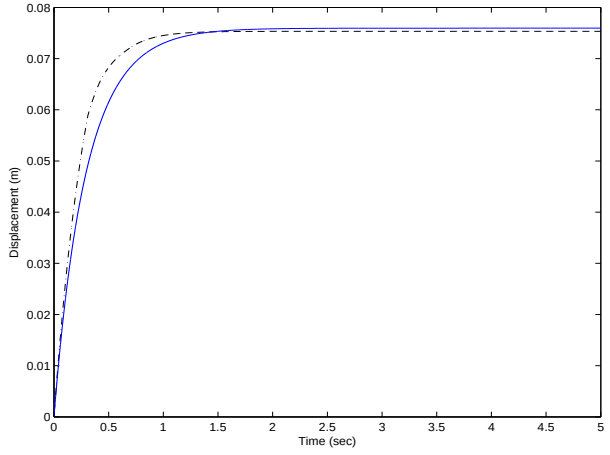

Fig. 11. Step Response for pressure $P = 6bar$

noted that among the responses of the non–linear model and the corresponding switched systems, only a small and almost negligible tracking error has been noticed in the proposed approach. This deviation is being inserted primarily: a) from the number of the utilized switched systems N, and b) on the approximation towards the calculation of the $B(P)$ and $K(P)$ parameters from the experimental measurements.

V. Conclusions

In this paper a switched system modeling of a PMA was presented. Given the phenomenological model of a PMA and the assumption of a vertically positioned PMA with a load attached to the loose end, a non linear model was extracted. Following a rough experimental estimation of the spring and damping coefficient relations for the muscle, a

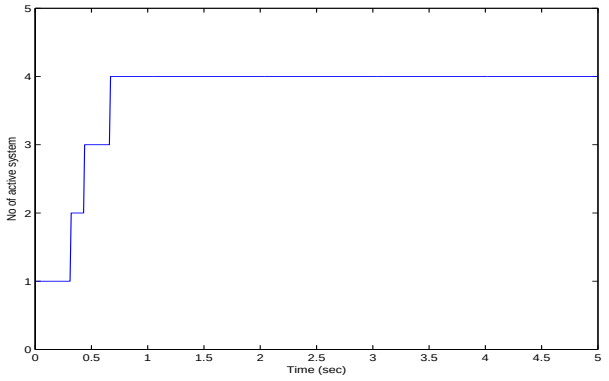

Fig. 12. Switched system activation for pressure $P = 6bar$

switched system model approach was considered. A trade–off has been done in both the estimation of the K and B parameters - by ignoring the inertial term $M\ddot{x}$ - and in the number of on switched systems, on account of simpler experimental setup and linear representation of the overall scheme. The said system was compared with the non linear model, resulting in a satisfactory linear approach. The resulting linearization can be improved by the further increase in the number of the switching systems. As future work, an accurate identification of the spring and damping coefficients can be a achieved, for benchmarking the switched system with the real muscle.

References

[1] D. Caldwell, G. Medrano-Cerda, and M. Goodwin, "Braided pneumatic actuator control of a multi-jointed manipulator," in *Proceedings of the IEEE International Conference on Systems, Man and Cybernetics*, Le Touquet, 1993, pp. 423–428.

[2] V. Nickel, J. Perry, and A. Garrett, "Development of useful function in the severely paralyzed hand," *Journal of Bone and Joint Surgery*, vol. 45-A, no. 5, pp. 933–952, 1963.

[3] H. Schulte, "The characteristics of the McKibben Artificial Muscle," in *The Application of External Power in Prosthetics and Orthotics*, Lake Arrowhead, 1961, pp. 94–115.

[4] G. K. Klute and B. Hannaford, "Modeling Pneumatic McKibben Artificial Muscle Actuators: Approaches and Experimental Results," *ASME Journal of Dynamic Systems, Measurements, and Control*, 1999.

[5] ——, "Accounting for elastic energy storage in McKibben artificial muscle actuators," *ASME Journal of Dynamic Systems, Measurement and Control*, pp. 386–388, 2000.

[6] J. Yarlott, "Fluid actuator ," *US Patent No. 3 645 173*, 1972.

[7] D. Caldwell and N. Tsagarakis, "Biomimetic actuators in prosthetic and rehabilitation applications," *Technology and Health Care*, pp. 107–120, 2002.

[8] R. Pierce, "Expansible cover," *US Patent No. 2211478*, 1940.

[9] P. Desmaroux, "Improvements on tubular membranes used as a servo motor," *French Patent No. 951885*, 1947.

[10] H. DeHaven, "Tensioning device for producing a linear pull," *US Patent No. 2483088*, 1949.

[11] P. Warszawska, "Artificial pneumatic muscle," *Dutch patent No. 6704918*, 1967.

[12] B. Hannaford and J. M. Winters, "Actuator properties and movement control: biological and technological models," in *Multiple Muscle Systems: Biomechanics and Movement Organization*, New York, 1990, pp. 101–120.

[13] E. Kelasidi, G. Andrikopoulos, G. Nikolakopoulos, and S. Manesis, "A Survey on Pneumatic Muscle Actuators Modeling," in *20th IEEE International Symposium on Industrial Electronics (ISIE 2011)*, Gdansk, Poland, 2011.

[14] G. Andrikopoulos, G. Nikolakopoulos, and S. Manesis, "A survey on Applications of Pneumatic Artificial Muscles," *accepted for publication in the 19th Mediterranean Conference on Control and Automation, June 20-23, Corfu, Greece*, 2011.

[15] C. Chou and B. Hannaford, "Measurement and modeling of McKibben pneumatic artificial muscles," *Measurement and modeling of McKibben pneumatic artificial muscles*, vol. 12, no. 1, pp. 90–102, 1996.

[16] B. Tondu and P. Lopez, "Modeling and control of McKibben artificial muscle robot actuators," *IEEE Control Systems Magazine*, vol. 20, no. 2, pp. 15–38, 2000.

[17] F. Daerden, D. Lefeber, and P. Kool, "Using Free Radial Expansion Pneumatic Artificial Muscles to control a 1DOF robot arm," in *Proceedings of the First International Symposium on Climbing and Walking Robots*, Brussel, 1998, pp. 209–214.

[18] A. Pujana-Arrese, J. Arenas, I. Retolaza, A. Martinez-Esnaola, and J. Landaluze, "Modelling in Modelica of a pneumatic muscle: application to model an experimental set-up. ," in *In: 21st European conference on modelling and simulation*, 2007.

[19] F. Daerden, B. Verrelst, D. Lefeber, and P. Kool, "Controlling motion and compliance with Folded Pneumatic Artificial Muscles," in *Proceedings of the Second International Conference on Climbing and Walking Robots*, Portsmouth, 1999, pp. 667–677.

[20] J. Zhang, C. Yang, Y. Chen, Y. Zhang, and Y. Dong, "Modeling and control of a curved pneumatic muscle actuator for wearable elbow exoskeleton," *Mechatronics*, pp. 448–457, 2008.

[21] D. Reynolds, D. Repperger, C. Phillips, and G. Bandry, "Modeling the dynamic characteristics of pneumatic muscle," *Annals of Biomedical Engineering*, vol. 31, pp. 310–317, 2003.

[22] J. Serres, "Dynamic characterization of a pneumatic muscle actuator and its application to a resistive training device," Ph.D. dissertation, Wright State University, 2008.